

## Spontaneous breaking of minimal surface condition: Labyrinths in free standing smectic films

Damian Pocięcha<sup>1,\*</sup>, Ewa Gorecka<sup>1</sup>, Nataša Vaupotič<sup>2,3</sup>, Mojca Čepić<sup>2</sup>, Jozef Mieczkowski<sup>1</sup>

<sup>1</sup>Department of Chemistry, Warsaw University, Al. Zwirki i Wigury 101, 02-089 Warsaw, Poland. e-mail: pociu@chem.uw.edu.pl

<sup>2</sup>Jozef Stefan Institute, Jamova 39, 1000 Ljubljana, Slovenia

<sup>3</sup>Faculty of Education, Koroška 160, 2000 Maribor, Slovenia

*Due to the surface tension liquids tend to minimize the surface area. The minimal surface condition applies also to the freely suspended films made of liquid crystals and as a result the islands and/or deepes that are formed during the drawing of the film are metastable and annealing of the film makes it uniform in thickness. However, in thin free standing films made of dimeric molecules in the smectic phase the minimal surface area condition may be broken and the film surface area suddenly starts to increase, upon lowering the temperature. The periodic modulation of the film thickness is obtained and in result the most fascinating labyrinth structure of crests and valleys is formed.*

Periodic morphologies are omnipresent in soft matter physics. Relevant examples can be found among liquid crystals<sup>1-7</sup>, polymers<sup>8-11</sup>, superconductors<sup>12-13</sup>, magnetic thin layers<sup>14</sup>, magnetic fluids<sup>15</sup>, biological membranes<sup>16</sup> etc. Formation of spatially modulated superstructure is manifestation of a competition between opposite forces governing organization in these systems. In the simplest case a stripe pattern is formed, but also more complicated 2-D or 3-D structures can develop, with square, honey-comb, spiral, labyrinth or gyroid lattices. Formation of complex patterns attracts considerable attention from both scientific and technological standpoints since they can be used as templates to fabricate devices at the nanometer-length scale<sup>17</sup>. It is common that the origin of the complex morphology is competition between the interactions at the surface and in the bulk, as in some systems they are much different<sup>18-20</sup>. The model systems to observe spatial instabilities driven by the competition between surface and bulk are thin layers of liquid crystals (LCs), for which the high surface area-to-volume ratio could be easily obtained. Additionally, fluidity of LCs makes them highly susceptible to instabilities.

Here we present experimental evidence of a system in which the minimal surface area condition is broken. Thin free standing films made of dimeric molecules forming the smectic liquid crystal phases were studied. Upon lowering the temperature a sudden increase in the surface area of the film occurs. This manifests itself in the periodic spatial modulation of the film thickness and the formation of an unusually beautiful stripe-labyrinth pattern.

We suggest that the spontaneous increase of surface area is driven by the difference in the density in the surface and bulk layers. Although applied to the special class of mesogenic compounds - dimeric molecules, forming intercalated lamellar phases, in which the surface area has significantly lower density than the interior of the film - the mechanism should also be valid for a broader class of materials, including the *bent-shaped* mesogens, materials intensively studied over the last years<sup>21</sup>. Indeed formation of the labyrinth structure has been recently reported also for the polarisation modulated smectic C phase (B<sub>7</sub>)<sup>22</sup>. We can not exclude that similar mechanism is important also for some liotropic systems. If the molecules exhibit significantly different cross sections of hydrophilic and hydrophobic groups the undulated structure of the liotropic L<sub>β</sub> phase<sup>23-25</sup> might become favorable.

The dimeric compounds studied have three-ring mesogenic cores linked through the malonate unit, material **1**, or through the hydrogen bonding of terminal OH groups, material **2** (Fig. 1).

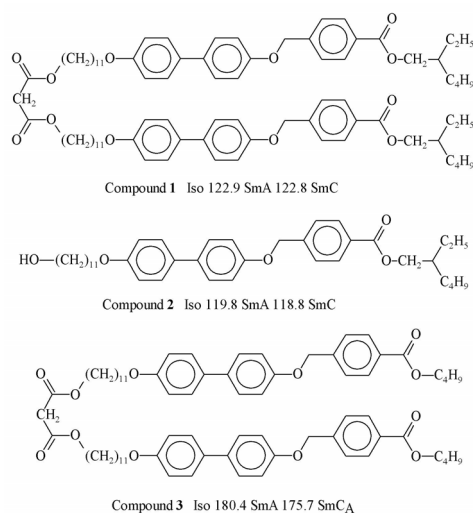


**Figure 1. Chemical formulas of the studied materials and the phase transition temperatures.**

The structure of the compounds in bulk was determined by the X-ray and the optical measurements. According to the X-ray measurements the compounds arrange in layers, the thickness of one layer being close to one half of the dimer length, which is characteristic to the intercalated structures. The optical measurements show that both compounds exhibit narrow temperature range of the smectic A (SmA) phase (the LC phase where molecules are on the average oriented in the direction of the smectic layer normal) and at lower temperatures the synclincic smectic C (SmC) phase (where the molecules are tilted away from the smectic layer normal and the tilt direction is the same in the neighbouring layers). No unusual behaviour within the temperature range of SmC phase was detected by the X-ray and optical methods.

However, in the freely suspended film samples (typically from several to a few hundreds smectic layers) at a certain temperature  $T_s$  ( $T_s \sim 85$  °C and  $\sim 97$  °C in material **1** and **2**, respectively) within the SmC phase temperature range the thickness of the film spontaneously modulates and the labyrinth of crests and valleys develops (Fig. 2).

The film thickness variation is visible in reflected light because the reflected colours depend strongly on the film thickness. The sudden nucleation of the labyrinth (Fig. 2a), the co-existence of the modulated and the unmodulated textures and the temperature hysteresis of nucleation reminds of the first order phase transition. The texture in film, annealed at temperature below  $T_s$  for several minutes, has regular pattern with well defined periodicity (Fig. 2b). The periodicity depends on the film thickness, the thinner the film the smaller is the periodicity. However, the thickness dependence is stronger for thinner than thicker films, suggesting nonlinear dependence. Comparing the textures observed in the reflected and the transmitted (between crossed polarizers) light it can be shown that the film thickness variation is coupled to the spatial variation of the molecular orientation. In the SmC phase the director  $\mathbf{n}$ , defining the average molecular orientation (Fig. 3a), is tilted from the layer normal  $\mathbf{v}$  giving rise to the birefringence of the film.

The spatial distribution of the director  $\mathbf{n}$  can easily be visualized under the polarizing microscope. The light transmission depends on the orientation of the  $\mathbf{c}$ -vector (a unit vector in the direction of the projection of the director onto the smectic layer) with respect to the direction of the polarizer and the analyzer. In the regions with thickness gradient (bright stripes in left part of Fig. 4) the  $\mathbf{c}$ -vector is uniformly oriented and it is perpendicular to the thickness gradient direction.

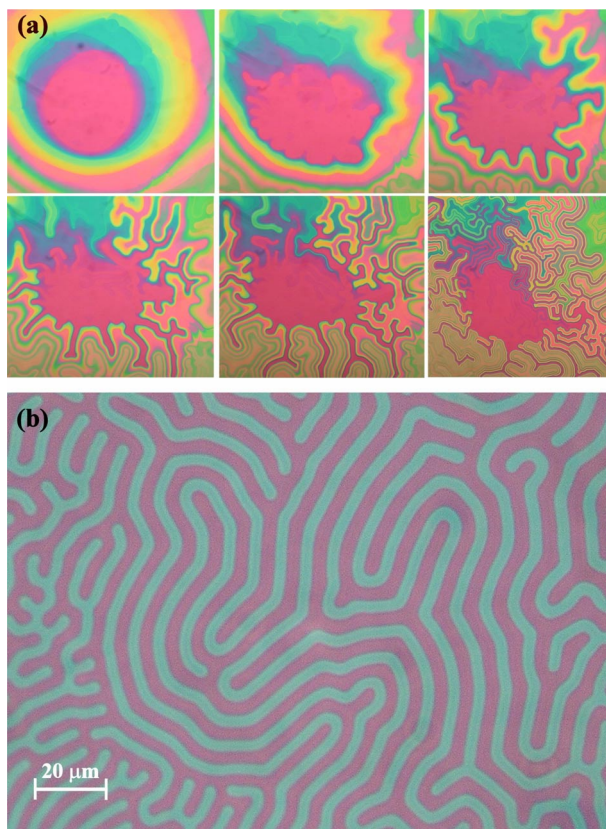


Figure 2. Freely suspended film of material 2 observed in the reflection mode. (a) the film region with strong thickness gradient, the central part is thinner than the outer part. Upon lowering the temperature (from 97.6 °C to 97.1 °C) the circular edge dislocation lines develop into the *labyrinth* structure. (b) enlarged part of the film annealed at  $T = 95$  °C.

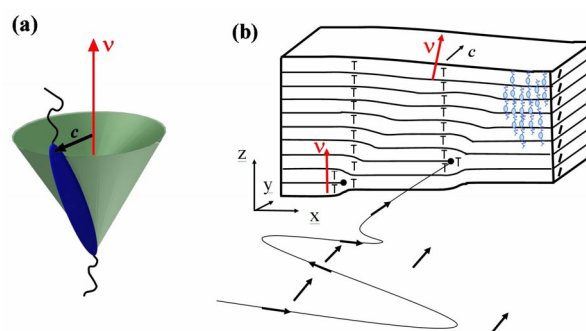
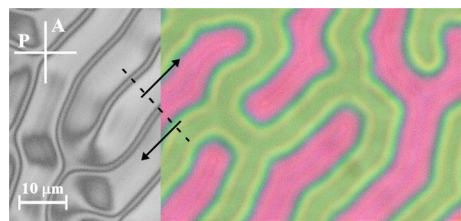
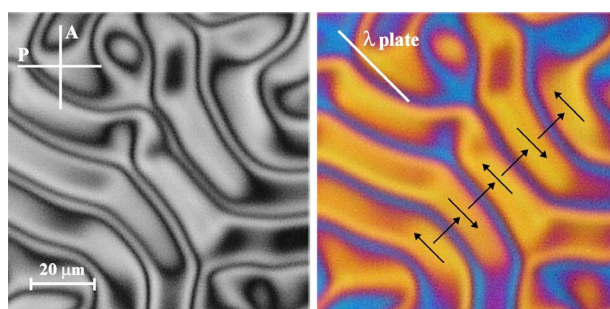


Figure 3. (a) The averaged position of molecule on the tilt cone in the SmC phase, the  $c$ -vector is the projection of the director  $n$  on the smectic plane and  $v$  is the layer normal. (b) Schematic drawing of the thickness gradient area in the freely suspended film of the SmC phase. The change of the film thickness requires the edge dislocations that are placed at some distance from the film surface, the elastic deformation is minimal if around each dislocation defect the director is tilted along the defect line ( $y$ -direction) and the  $c$ -vector is uniform through the film thickness. Such a structure enables additional tilt of the molecules in half-empty surface layer. Below certain temperature the edge dislocation lines start to curve giving rise to the stripe/labyrinth texture. The  $c$ -vector remains along the defect line and has to rotate by  $\pi$  between the neighbouring edge dislocation lines.



**Figure 4.** Freely suspended film of material 2 at  $T = 96$  °C, left side is observed between crossed polarizers in transmission mode, while the right side is observed without polarizers in reflection mode. The interference colours observed in reflection are due to the variation of the film thickness, pink/green corresponds to 520/440 nm. The regions with uniformly oriented  $\mathbf{c}$ -vector (arrows) correspond to the film thickness gradient (dotted line) and the orientation of the  $\mathbf{c}$ -vector is perpendicular the direction of the thickness gradient.

In order to determine unambiguously the  $\mathbf{c}$ -vector field corresponding to the observed pattern few additional experiments were made. The first order retardation plate that adds a fixed optical path difference to the transmitted light (a  $\lambda$ -plate) was inserted between the sample and the polarizer, oriented at 45 degrees from the polarizer axis. The onset of colours shows that within each broad stripe the  $\mathbf{c}$ -vector is oriented along the stripe and in regions between the stripes the orientation is perpendicular to the stripe (Fig. 5). Tilting the sample (imposing the oblique light incidence) along the stripes shows that in the neighbouring broad stripes the  $\mathbf{c}$ -vector has the opposite direction (Fig. 6), while tilting the sample in the direction perpendicular to the stripes shows that in the narrow regions between the broad stripes the  $\mathbf{c}$ -vector direction is identical. Thus it could be concluded that the  $\mathbf{c}$ -vector rotates by  $\pi$  between the stripes. The rotation is not uniform in space, the broad stripes with nearly uniformly oriented  $\mathbf{c}$ -vector are connected by narrow regions over which the  $\mathbf{c}$ -vector rotates ( $\pi$ -walls) and rotations in the negative and the positive sense interchange between the neighbouring stripes (Fig. 5). The  $\mathbf{c}$ -vector rotation takes place at tops of the crests and bottoms of the valleys of the film surface.



**Figure 5.** Stripe texture observed in the freely suspended film of material 1, at  $T = 80$  °C, between crossed polarizers (left), and with the  $\lambda$  plate inserted between the sample and the polarizer (right). Insertion of the  $\lambda$  plate parallel/perpendicular to the long axis of optical indicatrix increases/decreases the birefringence and thus shifts the birefringence colours to blue/yellow. Arrows indicate the direction of the  $\mathbf{c}$ -vector.

What is the possible mechanism for the observed instability which leads to the formation of the labyrinths in the presented system? Several compounds have been checked but the above described phenomenon is observed only for intercalated type tilted smectic phases. It should be noticed that in such system the surface layers are essentially “half empty”, which makes them energetically costly. The difference in the mass density between the surface and the bulk layers can be reduced by the deformation of the film surface. To decrease the intermolecular distances in the half empty surface layer and thus

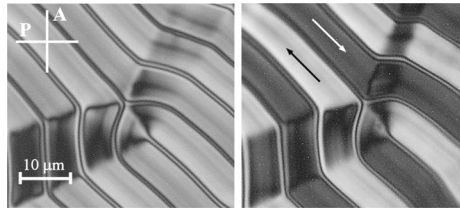


**Figure 6.** Stripe pattern in the freely suspended film of material 2 at  $T = 96$  °C, observed between crossed polarizers for normal light incidence (left) and for oblique light incidence (right). The oblique light incidence is obtained by tilting the film in the direction parallel to the stripes; this changes the orientation of the optical indicatrix in respect to the light propagation direction. The observed increase/decrease of birefringence indicates that the tilt direction alternates between stripes. Arrows show the c-vector direction.

reduce the surface free energy the surface layer inclines with respect to the interior of the film. Initially, the regions where the surface is inclined (sloped) are above the few edge dislocations (see Fig. 3b), which always exist in films with thickness islands. However, if at certain temperature system gains more in free energy from enlarging the sloped regions than it pays for elongation of the edge dislocation lines associated with increasing the sloped areas, the surfaces start to deform rapidly; this leads to the transition between the unmodulated and the modulated structure. Deformation of the film surface requires the flow of the material. The flow in liquid crystal is anisotropic<sup>26</sup>; it is the easiest in the direction of the **c**-vector. It is also known that the elastic deformation across the edge dislocation defect in the SmC phase is the smallest possible if the **c**-vector is tilted along the defect line<sup>27</sup> (*y*-direction in Fig. 3b). Thus the most efficient flow takes place tangentially to the dislocation line, this enhances the dislocation line curvature inhomogeneity and finally creates labyrinth pattern in the film (Fig. 2a). The initially approximately straight edge dislocation line begins to curl but the **c**-vector remains along the line. As a result, the **c**-vector has to rotate by  $\pi$  between the neighbouring edge dislocation lines, and the  $\pi$ -walls are formed (Fig. 3b). The periodicity of the stripes depends on the overall energy of the system that can be roughly estimated as:  $W = W_{edge}N + F_{int}d \exp\{-d_s / \lambda_\pi\} + W_\pi d + d_s W_s^{tilt}$ , where  $W_{edge}$  is the energy of a single edge dislocation line per unit length,  $N$  is the number of edge dislocation that depends on the thickness difference between two neighbouring film regions,  $W_\pi$  is the energy of  $\pi$ -wall per unit area,  $F_{int}$  gives the interaction energy over the distance  $d_s$  between two  $\pi$ -walls of the characteristic width  $\lambda_\pi$ , and  $W_s$  is the energy of the bent surface area. The  $\pi$ -wall energy increases linearly with increasing film thickness,  $d$ , the interaction energy between two  $\pi$ -walls decreases exponentially with the stripe width,  $d_s$ , and increases linearly with the film thickness, the surface energy increases linearly with the stripe width. The net result of the free energy minimization, with respect to  $d_s$ , is that the stripe width is a logarithmic function of the film thickness, as suggested by experiment:  $d_s = \lambda_\pi \ln \frac{F_{int}d}{W_s \lambda_\pi}$ . In

the model the interactions between the edge defects were neglected, since they decay with a characteristic length which is of the order of the smectic layer thickness<sup>27</sup>, thus they can not affect the stripe width. The interaction between two  $\pi$ -walls, however, is more far ranged. The characteristic length  $\lambda_\pi$  can be expected to be rather large, particularly in the intercalated structure.

The appearance of the described modulated structure seems to be more probable for synclinic type smectic phases than for anticlinic type ones. In the later case the energy of the bent surface structure is higher due to higher energy of dislocation defects, which is proportional to the Burger vector of the defect<sup>28</sup>. Due to the two layer lattice periodicity in the anticlinic phase the lowest energy dislocation defect requires Burger vector equal to 2. Indeed the labyrinth nucleation was never observed for material 3, which is structurally similar, but it exhibits anticlinic SmC<sub>A</sub> phase.

To conclude, we have presented a system in which the minimal surface condition is broken. Since in the intercalated smectic films made of dimeric molecules the surface layer is half empty and thus energetically costly, the surface effect dominates over the bulk effect when temperature is low enough. In order to reduce the intermolecular distance in the surface layer the surface layer undulates. This is

achieved by a periodical modulation of the film thickness which leads to the formation of the striped labyrinth structure.

ACKNOWLEDGMENT The work was supported by KBN Grant No 4T09A 00425 and organic synthesis by RTN grant HPRN-CT-2002-00171.

## REFERENCES

1. Galerne, Y.; Najjar, R. *Phys. Rev. E* **2004**, *69*, 031706.
2. Chao, C.-Y.; Pan, T.-C.; Ho, J. T. *Phys. Rev. E*, **2003**, *67*, 040702.
3. MacLennan, J. E.; Sohling, U.; Clark, N. A.; Seul, M. *Phys. Rev. E* **1994**, *49*, 3207.
4. Tabe, Y.; Shen, N.; Mazur, E.; Yokoyama, H. *Phys. Rev. Lett.* **1999**, *82*, 759.
5. Gorecka, E.; Glogarová, M.; Lejcek, L.; Sverenyák, H. *Phys. Rev. Lett.* **1995**, *75*, 4047.
6. Pang, J.; Clark, N. A. *Phys. Rev. Lett.* **1994**, *73*, 2332.
7. Lavrentovich, O. D.; Pergamenschik, V. M. *Phys. Rev. Lett.* **1994**, *73*, 979.
8. Beckmann, J.; Auschra, C.; Stadler, R. *Macromol. Rapid. Commun.* **1994**, *15*, 67.
9. Lee, M.; Cho, B.-K.; Zin, W.-Ch. *Chem. Rev.* **2001**, *101*, 3869.
10. Elbs, H.; Drummer, C.; Abetz, V.; Krausch, G. *Macromolecules* **2002**, *35*, 5570.
11. Bailey, T. S.; Hardy, C. M.; Epps, T. H.; Bates, F. S. *Macromolecules* **2002**, *35*, 7007.
12. Blatter, G.; Feigel'man, M. V.; Geshkenbein, V. B.; Larkin, A. I.; Vinokur, V. M. *Rev. Mod. Phys.* **1994**, *66*, 1125.
13. Kim, P.; Yao, Z.; Lieber, C. M. *Phys. Rev. Lett.* **1996**, *77*, 5118.
14. Seul, M.; Wolfe, R. *Phys. Rev. A* **1992**, *46*, 7519.
15. Jiang, I. M.; Tsai, M. S.; Lu, C. K.; Shih, C. C.; Chiang, J. C.; Horng, H. E. *Appl. Phys. Lett.* **2004**, *84*, 245.
16. Rozovsky, S.; Kaizuka, Y.; Groves, J. T. *J. Am. Chem. Soc.* **2005**, *127*, 36.
17. Yablonovitch, E. *Nature* **1999**, *401*, 539.
18. Singer, S. J. *Phys. Rev. E* **1993**, *48*, 2796.
19. Pereira, G. G.; Williams, D. R. M. *J. Chem. Phys.* **1999**, *110*, 9223.
20. Langer, S. A.; Sethna, J. P. *Phys. Rev. A* **1986**, *34*, 5035.
21. Niori, T.; Sekine, F.; Watanabe, J.; Furukawa, T.; Takezoe, H. *J. Mater. Chem.* **1996**, *6*, 1231.
22. Coleman, D. A.; Fernsler, J.; Chattham, N.; Nakata, M.; Takanishi, Y.; Korblova, E.; Link, D. R.; Shao, R. F.; Jang, W. G.; MacLennan, J. E.; Mondainn-Monval, O.; Boyer, C.; Weissflog, W.; Pelzl, G.; Chien, L.-C.; Zasadzinski, J.; Watanabe, J.; Walba, D. M.; Takezoe H.; Clark, N. A. *Science*, **2003**, *1204*, 301..
23. Wack, D. C.; Webb, W. W. *Phys. Rev. A* **1989**, *40*, 2712.
24. Sun, W.-J.; Tristram-Nagle, S.; Suter, R. M.; Nagle, J. F. *Proc. Natl. Acad. Sci. USA* **1996**, *93*, 7008.
25. Katsaras, J.; Tristram-Nagle, S.; Liu, Y.; Headrick, R. L.; Fontes, E.; Mason, P. C.; Nagle, J. F. *Phys. Rev. E* **2000**, *61*, 5668.
26. Carlsson, T.; Leslie, F. M.; Clark, N. A. *Phys. Rev. E* **1995**, *51*, 4509.
27. Hatwalne, Y.; Lubensky, T. C. *Phys. Rev. E* **1995**, *52*, 6240.
28. Takanishi, Y.; Takezoe, H.; Fukuda, A.; Watanabe, J. *Phys. Rev. B* **1992**, *45*, 7684.